

Noise in Digital and Digital-Analog Quantum Computation

Paula García-Molina,^{1,2,*} Ana Martín,¹ and Mikel Sanz^{1,3,4,†}

¹*Department of Physical Chemistry, University of the Basque Country UPV/EHU, Apartado 644, 48080 Bilbao, Spain*

²*Institute of Fundamental Physics, Calle Serrano 113b, 28006 Madrid, Spain*

³*IKERBASQUE, Basque Foundation for Science, Plaza Euskadi 5, 48009 Bilbao, Spain*

⁴*IQM, Nymphenburgerstr. 86, 80636 Munich, Germany*

Quantum computing makes use of quantum resources provided by the underlying quantum nature of matter to enhance classical computation. However, current Noisy Intermediate-Scale Quantum (NISQ) era in quantum computing is characterized by the use of quantum processors comprising from a few tens to, at most, few hundreds of physical qubits without implementing quantum error correction techniques. This limits the scalability in the implementation of quantum algorithms. Digital-analog quantum computing (DAQC) has been proposed as a more resilient alternative quantum computing paradigm to outperform digital quantum computation within the NISQ era framework. It arises from adding the flexibility provided by fast single-qubit gates to the robustness of analog quantum simulations. Here, we perform a careful comparison between digital and digital-analog paradigms under the presence of noise sources. The comparison is illustrated by comparing the performance of the quantum Fourier transform algorithm under a wide range of single- and two-qubit noise sources. Indeed, we obtain that, when the different noise channels usually present in superconducting quantum processors are considered, the fidelity of the QFT algorithm for the digital-analog paradigm outperforms the one obtained for the digital approach. Additionally, this difference grows when the size of the processor scales up, constituting consequently a sensible alternative paradigm in the NISQ era. Finally, we show how the DAQC paradigm can be adapted to quantum error mitigation techniques for canceling different noise sources, including the bang error.

I. INTRODUCTION

The origin of quantum computing dates back to 1980, when Benioff [1] suggested the use of quantum systems for traditional (reversible) computation, implementing a Turing-machine equivalence to unitary evolution. Simultaneously Manin [2], and a couple of years later Feynman [3], pointed out the convenience of quantum simulators to reproduce quantum problems. It was not until 1985 when Deutsch [4] proposed the idea of quantum gate, which led to the gate-based quantum computation model, known as the digital quantum computing (DQC) paradigm.

DQC is based on the use of digital pulses to perform quantum operations on the qubits, represented by means of single-qubit gates (SQG's), two-qubit gates (TQG's), and measurements. While DQC is the most outspread paradigm, there are other alternatives based on analog resources. One of the most promising ones is called adiabatic quantum computation or quantum annealing [5, 6]. Besides these paradigms, digital-analog quantum computing (DAQC) is created from merging the digital and analog paradigms, combining the adaptability of DQC with the robustness of analog resources [7]. This universal paradigm is based on the application of digital and analog blocks to implement quantum circuits in a quantum computer. The digital steps consist of SQG's, while analog blocks are constructed via the time evolution of the natural interacting Hamiltonian provided by the quantum processor. There are several works that employ this paradigm either to simulate quantum many body systems [8, 9] or to implement long depth quantum algorithms [10, 11].

Since the inception of quantum computing, a great deal of effort has been put into the development of the area. There is a great variety of hardware backends suitable for the performance of quantum computation, such as trapped ions [12] or superconducting circuits. The latest stands out as one of the most promising techniques to construct a quantum computer. They are solid-state electric circuits which use Josephson tunnel junctions, a highly non-linear and non-dissipative circuit element at low temperatures [13].

Noise is undoubtedly the main drawback in the scalability of quantum computing. Indeed, quantum computers cannot be completely isolated from the environment and the interactions performing quantum operations cannot be fully controlled, leading to decoherence, control errors and crosstalk. Due to the limitations imposed by these error sources, a huge effort has been made to analyze error sources and propose quantum protocols more resistant to them or capable of mitigating their effects [14, 15]. The most promising long-term solution for the scalability of quantum computers is the use of quantum error correction techniques [16, 17]. However, the Noisy Intermediate-Scale Quantum (NISQ) [18] era technology is not sufficient to implement quantum error correction to eliminate the undesired effect of noise sources in them.

A possibility to reduce the effect of noise sources in the era of NISQ devices is to adapt the quantum computing paradigm. Although the gate-based approach is the most extended paradigm, it is highly affected by noise. However, the effect is different depending on the type of gate. Indeed, it is almost negligible in SQG's, since they are fast and highly controllable. The length of TQG's makes them more exposed to decoherence, which together with the errors introduced by the indirect control and the crosstalk among qubits, turn these gates to be very sensitive to noise. DAQC emerges as a sensible alternative quantum paradigm to overcome this problem within the NISQ era limitations. This paradigm employs the

* Corresponding author: paula.garcia@iff.csic.es

† Corresponding author: mikel.sanz@ehu.es

natural interaction of the quantum processor to perform entangling operations and the running time of this Hamiltonian as an extra resource [19]. Consequently, the crosstalk among qubits and the control errors associated with switching on and off interactions are no longer a source of noise, but a resource, turning the problem of noise in TQG's into an advantage. Indeed, this approach has been numerically demonstrated to be more advantageous under the effect of certain experimental noise sources when compared to DQC [10]. However, in order to determine if DAQC is actually a suitable alternative to DQC in the NISQ era, a complete comparison of the performance of these paradigms comprising most of the noise sources present in superconducting quantum computers must be carried out.

In this Article, we perform a detailed comparison of the performance of DQC and DAQC paradigms under a wide range of noise sources, including thermal decoherence, bit-flip, measurement errors, and control errors. We illustrate it with the quantum Fourier transform, which is an important quantum subroutine with applications in multiple quantum algorithms [20–24]. The numerical study is performed for quantum processors of up to 6 qubits comparing the fidelity of the resulting state of the different paradigms with respect to the exact solution. The results conclude that the banded DAQC paradigm shows a better tolerance to the most relevant noise sources present in superconducting quantum computers. This improvement becomes more relevant when the number of qubits scales up, allowing in principle for a more accurate implementation of quantum algorithms in the NISQ era when compared to DQC.

We have organized the structure of the manuscript as follows. We start by explaining the fundamentals of DAQC in section II. In section III, we introduce the theoretical description of some of the most relevant noise sources present in current superconducting quantum computers. The comparison between the performance of DQC and DAQC is carried out in section IV. In section V, we successfully apply error mitigation techniques to the DAQC paradigm, which allow us to cancel both decoherence and bang errors. Finally, in section VI, the conclusions and future perspectives of this work are discussed.

II. DIGITAL-ANALOG QUANTUM COMPUTING

In Ref. [7], Parra-Rodriguez *et al.* introduced a paradigm of quantum computation called DAQC. A DAQC algorithm combines elementary SQG's, performed with high accuracy with current technology, with entangling natural interactions among qubits in the processor. In addition to superconducting circuits [25], this paradigm of computation can be straightforwardly adapted to other quantum platforms such as trapped ions [26], Rydberg atoms [27], or nuclear magnetic resonance [28, 29].

In a superconducting quantum processor, digital blocks are implemented by short microwave pulses, while the analog blocks are derived from the qubit-to-qubit capacitive or inductive coupling. This interaction depends on the type of coupling, the topology of the architecture or the nature of the

qubit, among other aspects, but it can be generally expressed as a spin Hamiltonian. In our case, for the sake of simplicity, we have chosen an homogeneous all-to-all (ATA) Ising Hamiltonian. Although, in the case that qubits were coupled by an arbitrary inhomogeneous nearest-neighbor Ising Hamiltonian, it is possible to generate an arbitrary all-to-all Ising Hamiltonian only by employing single-qubit rotations [30]

$$H_0 = H_{\text{int}} = g \sum_{j < k}^N Z^{(j)} Z^{(k)} \quad \rightarrow \quad U_{\text{int}}(t) = e^{itH_{\text{int}}}, \quad (1)$$

where g is the coupling constant among qubits and $Z^{(i)}$ is the Pauli matrix $\sigma_z^{(i)}$ applied on the i -th qubit. However, the DAQC paradigm can be adapted to other emergent Hamiltonians, resulting in a universal paradigm for essentially all of them.

The homogeneous ATA two-body Ising Hamiltonian is a particular case of the inhomogeneous version,

$$H_{ZZ} = \sum_{j < k}^N g_{jk} Z^{(j)} Z^{(k)}, \quad \text{with} \quad U_{ZZ} = e^{it_F H_{ZZ}}, \quad (2)$$

where now the coupling constant g_{jk} is different for each pair of qubits. For the sake of completeness, let us review the method introduced in Ref. [7]. Our first goal is to construct an arbitrary inhomogeneous Hamiltonian employing a combination of the aforementioned SQG's and analog blocks. Indeed, we can represent the evolution U_{ZZ} of an N -qubit inhomogeneous ATA two-body Ising Hamiltonian by $N(N-1)/2$ time slices U_{int} with times $\{t_{jk}\}_{j < k}^N$, where j, k are the indices of the application of the Z gates. More specifically, the analog block $U_{\text{int}}(t_{nm})$ is sandwiched by $X^{(n)} X^{(m)}$ rotations. The map between both pictures is

$$\begin{aligned} H_{ZZ} &= \sum_{j < k}^N g_{j,k} Z^{(j)} Z^{(k)} \\ &= \frac{g}{t_F} \sum_{j < k}^N \sum_{n < m}^N t_{nm} X^{(n)} X^{(m)} Z^{(j)} Z^{(k)} X^{(n)} X^{(m)}. \end{aligned} \quad (3)$$

Let us now see how the times t_{nm} must be chosen. Pauli matrices verify $\{\sigma_i, \sigma_j\} = 2\delta_{ij}\mathbb{I}$ for $i = x, y, z$, so for a term of the type $Z^{(k)} X^{(n)}$, it holds that $Z^{(k)} X^{(n)} = (-1)^{\delta_{kn}} X^{(n)} Z^{(k)}$, and analogously for the other terms. Using this we can write Eq. 3 as

$$H_{ZZ} = \frac{g}{t_F} \sum_{j < k}^N \sum_{n < m}^N t_{nm} (-1)^{\delta_{nj} + \delta_{nk} + \delta_{mj} + \delta_{mk}} Z^{(j)} Z^{(k)}. \quad (4)$$

This leads to a determined system of $N(N-1)/2$ linear equations, where the unknowns are the time steps of the analog blocks. The value of each time t_{nm} is given by the matrix inversion problem

$$g_{\beta} = t_{\alpha} M_{\alpha\beta} \frac{g}{t_F} \quad \rightarrow \quad t_{\alpha} = (M^{-1})_{\alpha\beta} g_{\beta} \frac{t_F}{g}, \quad (5)$$

where $M_{\alpha\beta}$ is a doubly stochastic matrix with elements ± 1 , $M_{\alpha\beta} = (-1)^{\delta_{nj} + \delta_{nk} + \delta_{mj} + \delta_{mk}}$. The new indexes α and β are introduced to vectorize each pair of indexes (j, k) and (n, m) as

$$\alpha = N(n-1) - \frac{n(n+1)}{2} + m, \quad (6)$$

$$\beta = N(j-1) - \frac{j(j+1)}{2} + k. \quad (7)$$

This matrix is invertible $\forall N \in \mathbb{Z} - \{4\}$ [8].

The method described is called stepwise DAQC (sDAQC) and it is universal and, therefore, equivalent to DQC. However, it shows the disadvantage that the analog blocks must be switched on and off, which induces important control errors. There is another paradigm called banged DAQC (bDAQC) in which the interaction Hamiltonian is never switched off and SQR's are applied on top of the analog dynamics. This introduces an inherent error, since it does not implement the exact algorithm, but when experimental errors are taken into account, it happens to scale up better than sDAQC and DQC [10, 11, 21]. This intuitively holds when the application time of SQRs, Δt , is much smaller than the time scale of the analog blocks, so the error introduced is smaller than the one coming from switching on and off the Hamiltonian in sDAQC. Indeed, experimentally, switching the interaction is not an exact step function and it takes some time to stabilize. A scheme of the implementation of both sDAQC and bDAQC is shown in Fig. 1.

III. THEORETICAL DESCRIPTION OF THE EFFECT OF NOISE SOURCES IN QUANTUM SYSTEMS

Quantum computers are open quantum systems, i.e., they cannot be completely isolated from the environment, and thus, they are susceptible to the noise caused by the control and the interaction with the environment. In general, the noise sources depend on the experimental setup used to run the quantum experiments. Our theoretical treatment of noise will employ the quantum channel formalism, in particular the operator-sum representation. In this formalism, the state of a quantum system is represented by a density matrix ρ . The general description of a quantum channel is a linear application, a completely-positive-trace-preserving map \mathcal{E} , which maps the initial state ρ into the final one ρ' , i.e.,

$$\rho' = \mathcal{E}(\rho). \quad (8)$$

It encloses the change in the dynamics of the system by the application of an operator which describes a physical process [31]. These processes are, for example, the application of a quantum operation on a qubit or the de-excitation of a state due to the interaction with the environment.

The operator-sum representation is a rigorous mathematical formalism for quantum channels. Let us suppose that we have an open quantum system comprising our system of interest S and the environment E , with Hilbert spaces \mathcal{H}_S and \mathcal{H}_E , respectively, and $\{|e_k\rangle\}$ is an orthonormal basis for the finite-dimensional Hilbert space corresponding to the environment.

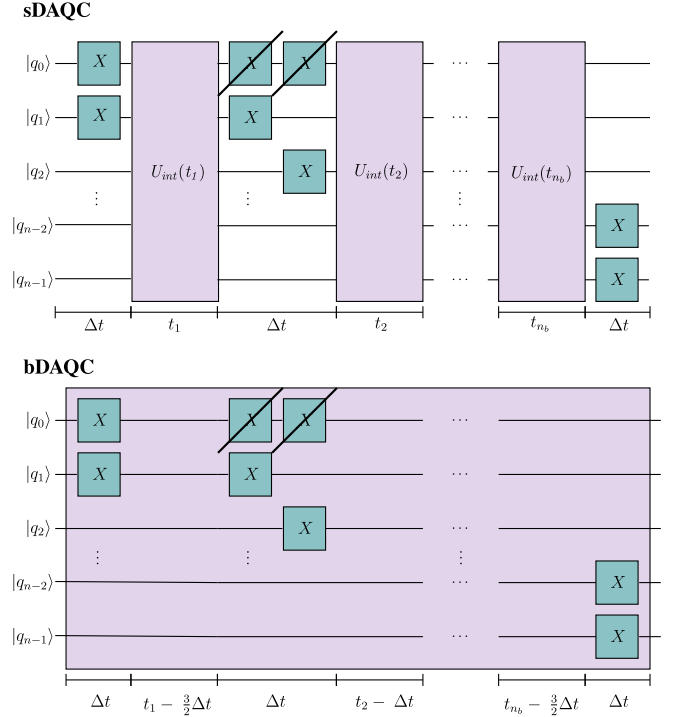


FIG. 1. **Scheme of the implementation of the sDAQC and bDAQC paradigms.** The analog blocks are depicted in purple and represent the interaction given by U_{int} in Eq. 1. The digital blocks are the blue ones, given by X gates. We can observe that in bDAQC, the digital blocks act on top of the analog interaction, while for sDAQC this interaction is turned on and off alternating with the digital blocks.

Let us assume that the initial state of the environment is $\rho_{\text{env}} = |e_0\rangle\langle e_0|$. For the transformation U , the quantum operation can be written as [31]

$$\begin{aligned} \mathcal{E}(\rho) &= \text{tr}_{\text{env}} [U (\rho \otimes |e_0\rangle\langle e_0|) U^\dagger] \\ &= \sum_k \langle e_k | U (\rho \otimes |e_0\rangle\langle e_0|) U^\dagger | e_k \rangle \\ &= \sum_k E_k \rho E_k^\dagger, \end{aligned} \quad (9)$$

where $E_k \equiv \langle e_k | U | e_0 \rangle$ is an operator which acts on the subspace of the system. The operators E_k are called Kraus operators [32] and they play a key role in the description of the effect of noise sources in quantum systems.

Noise channels are non-unitary quantum channels that reproduce the effect of noise in the state of the system of interest, in our case the qubits comprising a quantum computer. Let us first focus on single-qubit quantum channels, that are those that only act on one qubit. More concretely, we study the noise channels that account for the three most common noise sources in superconducting quantum processors. These are bit-flip, decoherence and measurement error.

The bit-flip channel is a model for errors in which the state of the qubit is randomly switched with a probability p and it is also present in classical computers. The energy to cause the

flip of the qubit can be accidentally provided by pulses used to control the qubits or by thermal fluctuations. The Kraus operators of the bit-flip channel are

$$E_0 = \sqrt{1-p} \begin{pmatrix} 1 & 0 \\ 0 & 1 \end{pmatrix} = \sqrt{1-p} \mathbb{I}, \quad (10)$$

$$E_1 = \sqrt{p} \begin{pmatrix} 0 & 1 \\ 1 & 0 \end{pmatrix} = \sqrt{p} X, \quad (11)$$

where p is the bit-flip probability, \mathbb{I} is the 2×2 identity matrix and X is the σ_x Pauli matrix. When the measurement of the system is performed, the qubits might be affected by a bit-flip error. Based on this idea, we will introduce the measurement error as a bit-flip error preceding a perfect measurement operation.

Decoherence is represented by means of the generalized amplitude-damping channel. This quantum channel accounts for the de-excitation of a two-level system, i.e., the loss of amplitude of the excited state $|1\rangle$ that will decay into the ground state $|0\rangle$ with probability p . It can describe different physical phenomena related to energy dissipation such as the spontaneous emission of a photon and the scattering and attenuation of the state of a photon in a cavity, among others [31]. The Kraus operators of the generalized amplitude-damping channel are

$$E_0 = \sqrt{p} \begin{pmatrix} 1 & 0 \\ 0 & \sqrt{1-\gamma} \end{pmatrix}, \quad (12)$$

$$E_1 = \sqrt{p} \begin{pmatrix} 0 & \sqrt{\gamma} \\ 0 & 0 \end{pmatrix}, \quad (13)$$

$$E_2 = \sqrt{1-p} \begin{pmatrix} \sqrt{1-\gamma} & 0 \\ 0 & 1 \end{pmatrix}, \quad (14)$$

$$E_3 = \sqrt{1-p} \begin{pmatrix} 0 & 0 \\ \sqrt{\gamma} & 0 \end{pmatrix}, \quad (15)$$

where the stationary state of the environment is

$$\rho_{\text{env}} = \begin{pmatrix} p & 0 \\ 0 & 1-p \end{pmatrix}, \quad (16)$$

with p the thermal population of the ground state.

The damping process can be understood as a time-accumulative problem, in which the probability grows with time [33]. It can be shown that γ can be written as $\gamma = 1 - e^{-t/T_1}$, where t is the time and T_1 is the thermal relaxation time and it describes processes due to the coupling of the qubit to its neighbors, which is a large system in thermal equilibrium at a temperature much higher than the one of the qubit [31].

Additionally, we also consider the control-related experimental errors described in Refs. [8, 10]. In this case, instead of a quantum-channel approach, we employ quantum trajectories [34]. The error due to SQG's is common to DQC and DAQC, as both use them as a resource to implement quantum algorithms. It simulates a uniform magnetic field

noise affecting the qubits. It is given by the parameter ΔB , a random variable from a uniform probability distribution $\Delta B \in \mathcal{U}(-r_D \Delta t/2, r_D \Delta t/2)$, where $\mathcal{U}(a, b)$ stands for an uniform noise distribution with range boundaries (a, b) . The deviation ratio is given by r_D . This can be modeled as

$$e^{i\theta_k Z} \rightarrow e^{i\theta_k \Delta B Z}, \quad (17)$$

where Z stands for any SQG and θ_k is the rotation angle.

The noise due to the interaction among qubits is modeled in a different manner for DQC and DAQC. In DQC, any TQG can be decomposed in terms of CZ gates and SQG's. As the CZ gate can be written in terms of SQG's and ZZ interactions of the type described in Eq. 22, the effects of noise in any TQG can be modeled using the magnetic field noise for SQG's and a Gaussian phase noise for the two-qubit ZZ interaction. This Gaussian phase noise is represented by a random parameter $\varepsilon \in \mathcal{N}(0, \sigma_D)$ affecting the phase of the interaction, where $\mathcal{N}(\mu, \sigma)$ stands for a Gaussian distribution with mean μ and standard deviation σ . Its effect on a fixed $\pi/4$ phase interaction, which is usually the interaction of a digital quantum computer, is described by the change

$$e^{i\frac{\pi}{4} ZZ} \rightarrow e^{i\frac{\pi}{4}(1+\varepsilon)ZZ}. \quad (18)$$

For the DAQC paradigm, a Gaussian coherent noise affecting the time of the analog blocks is introduced to simulate the control error. It produces a switch in the time from $t_\alpha \rightarrow t_\alpha + \delta$, where $\delta \in \mathcal{N}(0, r_b \Delta t)$, with r_b the deviation ratio of the time Δt required for a single-qubit rotation. This can be implemented as

$$e^{it_\alpha H_{\text{int}}} \rightarrow e^{i(t_\alpha + \delta) H_{\text{int}}}, \quad (19)$$

where H_{int} is the natural interacting Hamiltonian of the quantum processor.

The parameters ε , ΔB and δ must be chosen for each case and individually adapted to the different situations. The Gaussian coherent phase noise has a greater value for sDAQC than for bDAQC, as a result of the effect of switching on and off the interaction in sDAQC, as explained in section II. The value of these parameters changes each time a gate is applied to the circuit, as the effects of the noise described can vary in each application.

IV. IMPLEMENTATION OF A NOISE MODEL USING THE DQC AND DAQC PARADIGMS

In this section, we illustrate the noise model described in section III with the quantum Fourier transform (QFT). In Ref. [10] is shown that the N-qubit QFT can be written as a series of unitary gates of the form

$$U_{\text{QFT}} = \left[\prod_{m=1}^{N-1} U_{\text{SQG},m} U_{\text{TQG},m} \right] \cdot U_{H,N}, \quad (20)$$

where

$$U_{\text{SQG},m} = \exp \left[i \sum_{k=2}^{N-(m-1)} \theta_k \left(\mathbb{I} - Z^{(k+m-1)} - Z^{(m)} \right) \right] \times \exp \left[\frac{i\pi}{2} \left(\mathbb{I} - \frac{Z^{(m)} + X^{(m)}}{\sqrt{2}} \right) \right], \quad (21)$$

$$U_{\text{TQG}} = \exp \left(i \sum_{c < k}^N \alpha_{c,k,m} Z^{(c)} \otimes Z^{(k)} \right), \quad (22)$$

$$U_{H,m} = \exp \left(\frac{i\pi}{2} \left[\mathbb{I} - \frac{(Z^{(m)} + X^{(m)})}{\sqrt{2}} \right] \right), \quad (23)$$

$$\theta_k = \frac{\pi}{2^{k+1}} \quad \text{and} \quad \alpha_{c,k,m} = \delta_{c,m} \frac{\pi}{2^{k-m+2}}, \quad (24)$$

where the superindices in brackets determine onto which qubit the gate acts. In order to obtain the total unitary, we compute the tensor product with the identity until dimension 2^N is reached.

The entangling gates of the algorithm are described by Eq. 22, which is the unitary representation of an inhomogeneous ATA two-body Ising Hamiltonian. The DQC paradigm decomposes the entangling gate into fixed $\pi/4$ phase inhomogeneous ATA two-body Ising Hamiltonians as

$$e^{i\alpha_{c,k,m} Z^c Z^k} = e^{i\frac{\pi}{4} Y^c} e^{i\frac{\pi}{4} Z^c Z^k} e^{i\alpha_{c,k,m} Y^c} X^k \times e^{i\frac{\pi}{4} Z^c Z^k} X^k e^{-i\frac{\pi}{4} Y^c}, \quad (25)$$

where the phase $\alpha_{c,k,m}$ is the coefficient in Eq. 24.

To obtain a fair comparison of the performance of DQC, sDAQC and bDAQC for the implementation of the QFT, we choose a series of initial states from the family of states $|\psi_0\rangle = \sin \beta |W_N\rangle + \cos \beta |GHZ_N\rangle$, where $\beta \in [0, \pi]$. The comparison is performed for the 3-, 5- and 6-qubit QFT so we can observe the effect of the noise sources as the number of qubits increases.

The noise model that we consider encloses the most relevant noise sources in superconducting quantum computers: bit-flip, decoherence and measurement error, as well as control-related errors such as magnetic field fluctuations. However, the difference in the implementation of the entangling blocks in DQC and DAQC leads to a different experimental error associated to them, which is modeled as a Gaussian phase noise on the application time of the TQG's in DQC and the analog blocks in DAQC.

The figure of merit used for the comparison is the fidelity

$$F(\rho_{\text{ideal}}, \rho_{\text{noisy}}) = \left[\text{tr} \left(\sqrt{\sqrt{\rho_{\text{ideal}}} \rho_{\text{noisy}} \sqrt{\rho_{\text{ideal}}}} \right) \right]^2, \quad (26)$$

where ρ_{ideal} is the ideal state after the application of the QFT, while ρ_{noisy} is the resulting state when the noise model is implemented. The fidelity verifies $0 \leq F(\rho_{\text{ideal}}, \rho_{\text{noisy}}) \leq 1$, and the larger the values the more similar are ρ_{ideal} and ρ_{noisy} .

The values of the parameters used to simulate the different noise sources are chosen to model realistic NISQ superconducting devices. For the experimental errors described in

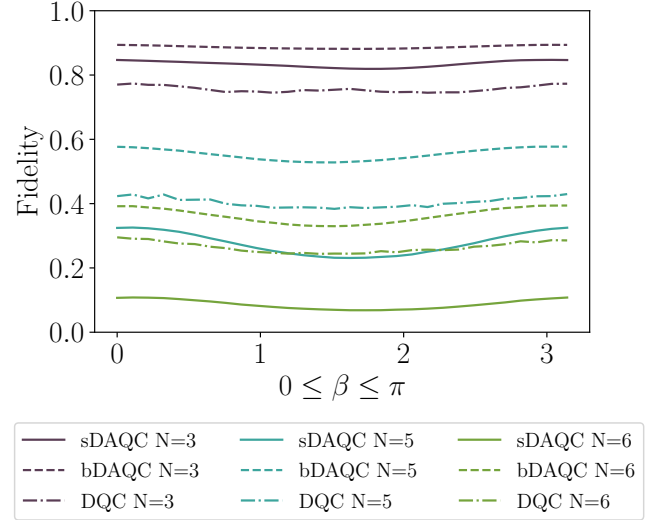


FIG. 2. **Fidelity of the implementation of the 3-, 5- and 6-QFT algorithm to the family of states $|\psi_0\rangle = \sin \beta |W_N\rangle + \cos \beta |GHZ_N\rangle$ using the the DQC, sDAQC and bDAQC paradigms.** The highest fidelity is obtained for the bDAQC protocol. DAQC presents a better tolerance to decoherence than DQC due to the shorter time of application of the analog blocks with respect to TQG's. Moreover, the effect of bit-flip error in bDAQC is smaller than on sDAQC as the analog interaction is always on, so the bit-flip only affects SQRs in bDAQC, as opposed to sDAQC in which all the qubits of the system are subjected to it when an analog block is applied.

Ref. [10], we select the values proposed by the authors. The magnetic field noise acting on single-qubit gates is given by a uniform probability distribution $\mathcal{U}(1 - \text{SQGN}, 1 + \text{SQGN})$, with $\text{SQGN} = 0.0005$. For the entangling blocks, for both DQC and DAQC the noise is modeled by a random variable from a Gaussian distribution $\mathcal{N}(0, \sigma)$. The value of the standard deviation σ depends on the paradigm used. For DQC, the standard deviation is $\text{TQGN} = 0.2000$, while for DAQC we have $\text{sABN} = 0.0200/g_0$ and $\text{bABN} = 0.0100/g_0$, for sDAQC and bDAQC, respectively. The parameter g_0 is the coupling constant of the homogeneous ATA two-body Ising Hamiltonian of the analog blocks and it is equal to 10 MHz. On the other hand, for the incoherent noise models introduced in Section III, we have a bit-flip error with probability $p_{\text{b-f}} = 0.005$ and a measurement error with probability $p_{\text{meas}} = 0.01$. Notice that measurement error is currently the technological limiting factor for quantum algorithms run in superconducting quantum processors. Finally, for the decoherence channel, the relaxation time T_1 is $50 \mu\text{s}$, with thermal population of the ground state $p = 0.35$. The length of the SQG's is $\Delta t_{\text{SQG}} = 1/(100g_0)$, while for the two-qubit interaction it is $\Delta t_{\text{TQG}} = (1 + \varepsilon)100\Delta t_{\text{SQG}}\pi/4$ for TQG's, and for the analog blocks, it is the one obtained from the decomposition of the interaction.

The simulation using the previous values of the parameters is depicted in Fig. 2, averaged over 1000 repetitions to obtain a sufficiently good statistical sample. We can conclude that

the bDAQC protocol shows a better performance when the noise sources considered by our noise model are taken into account. Although for the ideal case the lowest fidelity results are obtained for bDAQC [10], in the noisy simulation, we observe that it shows the best tolerance to errors. The reason is that the error due to turning on and off the interaction overcomes the inherent error of the bDAQC introduced by having the interaction always on. Moreover, the fact that the interaction is never switched off also makes bDAQC only affected by the bit-flip error for the SQG's, so no bit-flip error is introduced due to the entangling blocks as it does in both DQC and sDAQC. For the chosen set of parameters, the total time of application of the QFT algorithm using the DAQC paradigm is shorter than the total time using DQC. Therefore, the DAQC paradigm is less affected by decoherence than the DQC paradigm. The measurement error is common for the three paradigms, so its effect in the fidelity is reflected as a shift in all the values. The performance of the QFT algorithm decreases fast with the number of qubits due to the increase in depth of the algorithm, as the number of gates is of order $\mathcal{O}(N^2)$, where N stands for the number of qubits. Thus, under a fair comparison considering the experimental values and the same noise sources, bDAQC obtains the highest value of the fidelity.

Although we have chosen the QFT algorithm for our comparison, it allows us to extend the results to any general quantum algorithm, as the noise sources considered are independent of the algorithm implemented. In addition, if the scaling of the number of quantum gates with the number of qubits is slower than in the QFT, better fidelity results are expected.

V. ERROR MITIGATION IN DAQC

The effect of noise sources limits the performance of current NISQ processors [18]. Quantum error mitigation techniques emerge to successfully deal with these effects within the NISQ era [35, 36]. Therefore, in order to show the actual performance of DAQC, it is necessary to show how to adapt quantum error mitigation techniques to this paradigm. In fact, we will show that these techniques can be successfully modified to cancel the intrinsic error associated to bDAQC.

We apply the zero noise extrapolation technique [37, 38], based on the extrapolation of the noisy results to the zero noise limit. We consider only the effect of decoherence in the system and run the bDAQC QFT circuit for the initial state $|\psi_0\rangle = \sin \pi/4 |W_6\rangle + \cos \pi/4 |GHZ_6\rangle$, for different values of the coupling constant g_j , $j = 0, \dots, n_g$. This way, we modify the total time of the application of the circuit as $t_{j\alpha} \propto g_j^{-1}$ and hence, the effect of decoherence. However, the variation of g_j also affects the intrinsic error of the bDAQC paradigm. In order to avoid this effect, we choose $\Delta t_{\text{SQG}_{i,j}} = b_i/g_j$, as for a given g_j the time of the digital block is defined to be inversely proportional to the coupling constant. Then, for a certain number of values of g_j , it is possible to extrapolate the fidelity results to the zero decoherence limit-zero total time-, removing the error due to decoherence.

Moreover, it is also possible to extend this technique to

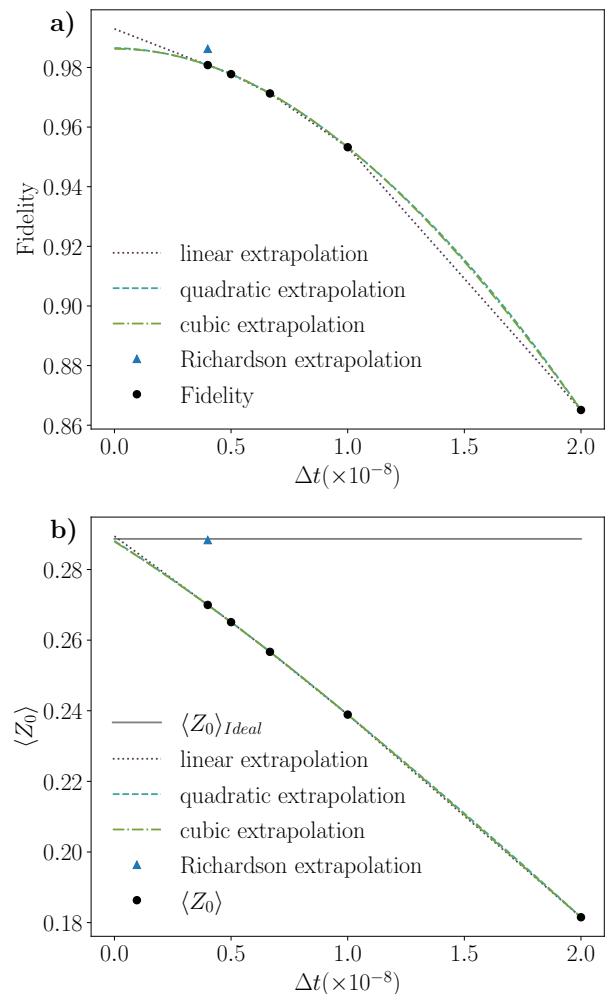


FIG. 3. **Results of the error mitigation. (a) Fidelity, and (b) $\langle Z_0 \rangle$.** Both fidelity and $\langle Z_0 \rangle$ attain extremely accurate approximations of the ideal values, especially for linear and Richardson extrapolation, respectively. The simulations were made for the 6-qubit QFT circuit with $T_1 = 50 \mu\text{s}$, $p = 0.35$ and $g_0 = 1 \text{ MHz}$.

eliminate the intrinsic error introduced by bDAQC. In order to do that, we repeat the previous procedure for $i = 0, \dots, n_t$ values of $\Delta t_{\text{SQG}_{i,j}} = b_i/g_j$, employing the zero decoherence values to perform the extrapolation to the zero Δt_{SQG} limit. The result is the fidelity of the ideal circuit, both without the error due to decoherence and bDAQC (Fig. 3a). The best fidelity is obtained for the linear extrapolation and it is approximately 0.9929, which means that the error mitigated state is a great approximation of the ideal one.

However, it is not always possible to obtain the quantum state after the application of a quantum circuit, as it is a costly operation due to the use of tomography. Thus, in order to verify the performance of error mitigation for bDAQC, it is necessary to choose a second figure of merit which can easily be computed from the measurements of a quantum circuit. We choose the expectation value of the observable $Z_0 = Z \otimes \mathbb{I} \otimes \dots \otimes \mathbb{I}$. The results are shown in Fig. 3b. We

observe that the best approximation of $\langle Z_0 \rangle$ is approximately 0.2883, computed using Richardson extrapolation. The error $\varepsilon = |\langle Z_0 \rangle_{\text{ideal}} - \langle Z_0 \rangle_{\text{noisy}}| = 0.0003$ shows that we can obtain an extremely accurate approximation of the ideal expectation value from the noisy one.

The results obtained in Fig. 3 show that it is possible to recover the ideal results from the application of the bDAQC paradigm by resorting to zero noise extrapolation. Although we have focused on bDAQC, these results can be extended to sDAQC, as in this case only the zero decoherence limit would be studied. For a more detailed discussion of the error mitigation for bDAQC and concrete results see the Appendix.

VI. CONCLUSIONS AND PERSPECTIVES

The aim of this manuscript was to perform an exhaustive platform-based comparison between the DAQC and DQC paradigms in order to determine if DAQC is actually a sensible alternative paradigm in the NISQ era. With this in mind, we have illustrated the experiment by implementing the QFT algorithm, considering a noise model that comprises the most relevant noise sources in current superconducting quantum processors. From our simulations, we conclude that bDAQC is a suitable alternative for NISQ processors. For 3 qubits the fidelity is about 90% for bDAQC and 85% for sDAQC, while for DQC it is about 80%. As the number of qubits increases, we have observed that the fidelity values obtained for bDAQC still overcome considerably the ones of DQC, al-

though sDAQC presents a worse performance, due to the increasing number of analog blocks affected by the bit-flip. For a higher number of qubits the effect of the noise sources leads to fidelity values too low to obtain conclusive results from the output of the experiments.

Moreover, we have also proven that quantum error mitigation techniques can be adapted to the DAQC paradigm, reinforcing the proposal of this paradigm as an appropriate alternative to DQC in the NISQ era.

The results are highly encouraging for the development of NISQ computation architectures. As an outlook, this study can be extended to consider other noise channels, such as correlated noises, in order to match the performance of other architectures [39, 40], as well as the comparison of our predictions with actual implementations based on transmon or flux qubits.

ACKNOWLEDGEMENTS

The authors thank Juan José García-Ripoll for the useful discussions. The authors acknowledge support from Spanish MCIU/AEI/FEDER (PGC2018-095113-B-I00), Basque Government IT986-16, the projects QMiCS (820505) and Open-SuperQ (820363) of the EU Flagship on Quantum Technologies, as well as the EU FET Open projects Quomorphic (828826) and Epicus (899368). P.G.M. acknowledges support from MCIU/AEI/FEDER PGC2018-094792-B-I00, CSIC Research Platform PTI-001, and FPU Grant FPU19/03590.

-
- [1] P. Benioff, *The computer as a physical system: A microscopic quantum mechanical Hamiltonian model of computers as represented by Turing machines*. Journal of Statistical Physics **22**, 563 (1980).
- [2] Y. I. Manin, *Vychislimoe i nevychislimoe*. Sov. Radio, 13 (1980).
- [3] R. P. Feynman, *Simulating physics with computers*. International Journal of Theoretical Physics **21**, 467 (1982).
- [4] D. Deutsch, *Quantum theory, the Church–Turing principle and the universal quantum computer*. Proceedings of the Royal Society A **400**, 97 (1985).
- [5] E. Farhi, J. Goldstone, S. Gutmann, and M. Sipser, *Quantum Computation by Adiabatic Evolution*. ArXiv: quant-ph/0001106 (2000).
- [6] T. Albash and D. A. Lidar, *Adiabatic quantum computation*. Rev. Mod. Phys. **90**, 015002 (2018).
- [7] A. Parra-Rodríguez, P. Lougovski, L. Lamata, E. Solano, and M. Sanz, *Digital-Analog Quantum Computation*. Physical Review A **101**, 022305 (2020).
- [8] L. Lamata, A. Parra-Rodríguez, M. Sanz, and E. Solano, *Digital-analog quantum simulations with superconducting circuits*. Advances in Physics: X **3** 1457981 (2018).
- [9] L. C. Céleri, D. Hueriga, F. Albarrán-Arriagada, E. Solano, and M. Sanz, *Digital-analog quantum simulation of fermionic models*. ArXiv: 2103.15689 (2021).
- [10] A. Martin, L. Lamata, E. Solano, and M. Sanz, *Digital-analog quantum algorithm for the quantum Fourier transform*. Physical Review Research **2**, 013012 (2020).
- [11] D. Headley, T. Müller, A. Martin, E. Solano, M. Sanz, and F. K. Wilhelm, *Approximating the Quantum Approximate Optimization Algorithm*. ArXiv:2002.12215 (2021).
- [12] J. I. Cirac and P. Zoller, *Quantum Computations with Cold Trapped Ions*. Physical Review Letters **74**, 4091 (1995).
- [13] M. H. Devoret, A. Wallraff, and J. M. Martinis, *Superconducting Qubits: A Short Review*. ArXiv:cond-mat/0411174 (2004).
- [14] Y. Zhang, H. Deng, Q. Li, H. Song, and L. Nie, *Optimizing Quantum Programs Against Decoherence: Delaying Qubits into Quantum Superposition*. 13th International Symposium on Theoretical Aspects of Software Engineering (TASE), July 29 – August 1, (2019).
- [15] M. Sarovar, T. Proctor, K. Rudinger, K. Young, E. Nielsen, and R. Blume-Kohout, *Detecting crosstalk errors in quantum information processors*. Quantum **4**, 321 (2020).
- [16] P. W. Shor, *Scheme for reducing decoherence in quantum computer memory*. Physical Review A **52**, 2493 (1995).
- [17] C. H. Bennett, D. P. DiVincenzo, J. A. Smolin, and W. K. Wootters, *Mixed-state entanglement and quantum error correction*. Physical Review A **54**, 3824 (1996).
- [18] J. Preskill, *Quantum Computing in the NISQ era and beyond*. Quantum **2**, 79 (2018).
- [19] T. Gonzalez-Raya, R. Asensio-Perea, A. Martin, L. C. Céleri, M. Sanz, P. Lougovski, and E. F. Dumitrescu, *Digital-Analog Quantum Simulations Using The Cross-Resonance Effect*. PRX Quantum **2**, 020328 (2021).
- [20] P. W. Shor, *Polynomial-Time Algorithms for Prime Factorization and Discrete Logarithms on a Quantum Computer*. SIAM

Journal on Computing **26**, 1484 (1996).

- [21] A. Martín, B. Candelas, Á. Rodríguez-Rozas, J. D. Martín-Guerrero, X. Chen, L. Lamata, R. Orús, E. Solano, and M. Sanz, *Toward Pricing Financial Derivatives with an IBM Quantum Computer*. Physical Review Research **3**, 013167 (2021).
- [22] J. Gonzalez-Conde, Á. Rodríguez-Rozas, E. Solano, and M. Sanz, *Pricing Financial Derivatives with Exponential Quantum Speedup*. ArXiv:2101.04023 (2021).
- [23] A. W. Harrow, A. Hassidim, and S. Lloyd, *Quantum Algorithm for Linear Systems of Equations*. Physical Review Letters **103**, 150502 (2009).
- [24] S. Lloyd, M. Mohseni, and P. Rebentrost, *Quantum principal component analysis*. Nature Physics **10**, 631 (2014).
- [25] J. Yu, J. C. Retamal, M. Sanz, E. Solano, and F. Albarrán-Arriagada, *Superconducting Circuit Architecture for Digital-Analog Quantum Computing*. ArXiv: 2103.15696 (2021).
- [26] D. Porras, and J. I. Cirac, *Effective Quantum Spin Systems with Trapped Ions*. Physical Review Letters **92**, 207901 (2004).
- [27] A. W. Glaetzle, R. M. W. van Bijnen, P. Zoller, and W. Lechner, *A coherent quantum annealer with Rydberg atoms*. Nature Communications **8**, 15813 (2017).
- [28] S. Lloyd, *A Potentially Realizable Quantum Computer*. Science **261**, 1569 (1993).
- [29] D. G. Cory, M. D. Price, and T. F. Havel, *Nuclear magnetic resonance spectroscopy: An experimentally accessible paradigm for quantum computing*. Physica D: Nonlinear Phenomena **120**, 82 (1998).
- [30] A. Galicia, B. Ramon, E. Solano, and M. Sanz, *Enhanced connectivity of quantum hardware with digital-analog control*. Physical Review Research **2**, 033103 (2020).
- [31] M. A. Nielsen and I. L. Chuang, *Quantum Computation and Quantum Information* (Cambridge University Press, Cambridge, 2010).
- [32] K. Kraus, *States, Effects and Operations: Fundamental Notions of Quantum Theory* (Springer Verlag, 1983).
- [33] J. Preskill, *Lecture Notes for Ph219/CS219: Quantum Computation Chapter 3* (California Institute of Technology, 2018).
- [34] H. J. Carmichael, *Quantum jumps revisited: An overview of quantum trajectory theory* (Quantum Future From Volta and Como to the Present and Beyond. Lecture Notes in Physics, vol 517. Springer, Berlin, Heidelberg, 1999).
- [35] S. Endo, S. C. Benjamin, and Y. Li, *Practical Quantum Error Mitigation for Near-Future Applications*. Physical Review X **8**, 031027 (2018).
- [36] A. Kandala, K. Temme, A. D. Córcoles, A. Mezzacapo, J. M. Chow, and J. M. Gambetta, *Error mitigation extends the computational reach of noisy quantum processor*. Nature **567**, 491 (2019).
- [37] Y. Li and S. C. Benjamin, *Efficient Variational Quantum Simulator Incorporating Active Error Minimization*. Physical Review X **7**, 021050 (2017).
- [38] K. Temme, S. Bravyi, and J. M. Gambetta, *Error Mitigation for Short-Depth Quantum Circuits*. Physical Review Letters **119**, 180509 (2017).
- [39] L. Postler, Á. Rivas, P. Schindler, A. Erhard, R. Stricker, D. Nigg, T. Monz, R. Blatt, and M. Müller, *Experimental quantification of spatial correlations in quantum dynamics*. Quantum **2**, 90 (2018).
- [40] A. Bermudez, X. Xu, M. Gutiérrez, S. C. Benjamin, and M. Müller, *Fault-tolerant protection of near-term trapped-ion topological qubits under realistic noise sources*. Physical Review A **100**, 062307 (2019).

Appendix: ERROR MITIGATION

In section V we demonstrated how to apply error mitigation to the DAQC paradigm. In this appendix we include a more detailed explanation of the procedure, as well as the values chosen for these simulations and the numerical results obtained.

First, in order to have a greater effect of the noise sources in our system, we choose $g_0 = 1$ MHz and only consider the effect of decoherence by means of the thermal relaxation channel with $T_1 = 50 \mu\text{s}$ and $p = 0.35$. We opt for a 6-qubit initial state $|\psi_0\rangle = \sin \pi/4 |W_6\rangle + \cos \pi/4 |\text{GHZ}_6\rangle$ and apply the bDAQC QFT circuit on it to study its fidelity and expectation value $\langle Z_0 \rangle$ for different values of $\Delta t_{\text{SQG}_{i,j}} = b_i/g_j$, with $b_i = [1/50, 1/100, 1/150, 1/200, 1/250]$ and $g_j = a_j g_0$, $a_j = [0.94, 0.97, 1.00, 1.03, 1.07]$.

The procedure is as follows. For each value of b_i , we perform a zero noise linear extrapolation with the time associated to each g_j as the noise parameter, leading to the zero decoherence limit for each b_i , i.e., $\Delta t_{\text{SQG}_i} = b_i/g_0$, for the fidelity and the expectation value $\langle Z_0 \rangle$ (see Tables I-II). Using the zero decoherence limit values of these figures of merit we can move on to the step two of the error mitigation for bDAQC, which is used to remove the intrinsic error associated to this paradigm. We use different extrapolation techniques and obtain the results in Tables III-IV.

	b_0	b_1	b_2	b_3	b_4
g_0	0.7270	0.8006	0.8156	0.8211	0.8236
g_1	0.7312	0.8052	0.8204	0.8258	0.8284
g_2	0.7352	0.8096	0.8249	0.8303	0.8329
g_3	0.7390	0.8138	0.8291	0.8346	0.8372
g_4	0.7437	0.8190	0.8344	0.8400	0.8426
Zero decoherence limit	0.8651	0.9532	0.9713	0.9778	0.9808
Ideal	0.8771	0.9665	0.9848	0.9914	0.9945

TABLE I. Fidelity results for the first step of the zero noise extrapolation for bDAQC (zero decoherence).

	b_0	b_1	b_2	b_3	b_4
g_0	0.1692	0.2185	0.2337	0.2409	0.2451
g_1	0.1696	0.2191	0.2344	0.2417	0.2459
g_2	0.1699	0.2197	0.2351	0.2424	0.2466
g_3	0.1703	0.2203	0.2357	0.2430	0.2473
g_4	0.1707	0.2210	0.2365	0.2439	0.2481
Zero decoherence limit	0.1815	0.2389	0.2567	0.2651	0.2700
Ideal	0.1813	0.2392	0.2571	0.2656	0.2705

TABLE II. $\langle Z_0 \rangle$ results for the first step of the zero noise extrapolation for bDAQC (zero decoherence).

Ideal	Linear	Cuadratic	Cubic	Richardson
1	0.9929	0.9865	0.9862	0.9862

TABLE III. Fidelity results for the second step of the zero noise extrapolation for bDAQC (zero Δt_{SQG}).

Ideal	Linear	Cuadratic	Cubic	Richardson
0.2887	0.2895	0.2881	0.2879	0.2883

TABLE IV. $\langle Z_0 \rangle$ results for the second step of the zero noise extrapolation for bDAQC (zero Δt_{SQG}).